Modeling the Response of Microdialysis Probes in Glucose Concentration Measurement

José M. Gozálvez-Zafrilla[1], Asunción Santafé-Moros*[1], José L. Díez-Ruano[2], Jorge Bondia[2]
[1]Institute for Industrial, Radiophysical and Environmental Safety (ISIRYM), Universitat Politècnica de Valencia
[2]Instituto Universitario de Automática e Informática Industrial (AI2), Universitat Politècnica de Valencia
* Chemical and Nuclear Engineering Department, Universitat Politècnica de Valencia,
C/ Camino de Vera s/n, 46022 Valencia, Spain, assanmo@iqn.upv.es

Abstract: Microdialysis is a technique useful for continuous glucose monitoring in diabetic patients. It is based on the transfer of glucose through a microdialysis membrane from the interstitial fluid to a saline solution perfused into the microdialysis probe. In this paper, a preliminary model for glucose transfer was developed for two types of microdialysis probes: a hollow-fiber using an inner cannula and a single hollow-fiber. The model was used to study the effects of the operating variables and the alterations due to the insertion of the microdialysis probe on the glucose measure.

Keywords: membrane, microdialysis, glucose.

1. Introduction

Microdialysis (MD) is an efficient technique of continuous glucose monitoring currently used in the glycemic control of type 1 diabetic patients [1]. Other important use of microdialysis is the study of pharmacokinetic and pharmacodynamics behavior of different agents as it allows the local administration of a substance and simultaneous sampling of the extracellular levels of compounds [2].

In MD, a saline serum is perfused into a hollow-fiber probe. Glucose pass from the plasmatic fluid through the porous membrane towards the perfusion solution as a consequence of the different glucose concentration existing between these two phases. The exiting perfused fluid constitutes the dialysate. The glucose concentration in the dialysate is measured by an external analytical device. The standard cut-off (lower molecular size that is rejected more than 95%) of MD membranes is 20 kD (20000 g/mol). This cut-off value assures that only small molecules like glucose pass to the dialysate, preventing the passage of proteins. Typical perfusing rates are in the range of 6- 300 µL/h to achieve enough dialysate production at easily measurable concentrations [3]. The perfusion solution must have ionic strength, osmotic pressure and pH values as close as possible to those of the extracellular fluid.

Figure 1 shows two typical configurations for a MD probe. In the cannula configuration, a porous hollow-fiber is inserted in the body. The saline solution is introduced to the tip of the hollow-fiber using an inner cannula. Then the solution flows in the space between the cannula and the MD membrane inserted in the body. In the other configuration a single hollow-fiber is inserted, the saline solution.

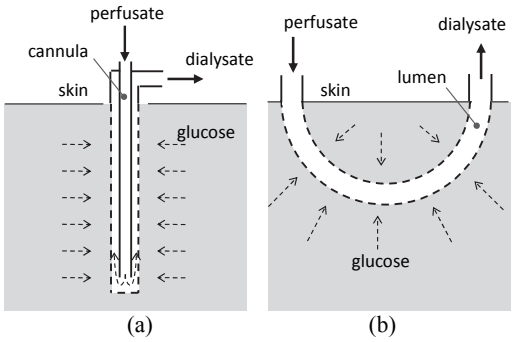

Figure 1. Studied configurations of microdialysis: I) hollow-fiber with inner cannula, II) hollow-fiber.

According to [4] among the characteristics required to glucose monitoring devices are:

- fast response: changes must be detected in less than 5 minutes
- accuracy: deviation < 0.5 mM
- sensitivity: 0.1 mM
- range: 1 to 30 mM
- stability: ±5% during operational time

The insertion of the probe causes an initial period of disturbed tissue function which can cause increased glucose metabolism, blood flow

changes, and other alterations. After 2 days, oedema, minor haemorrhages and leukocytes accumulation can occur [2]. These alterations can affect to the stability of the glucose measure.

2. Modeling

2.1 Modeling of the microdialysis probe

Some assumptions were made to simplify the geometry of both configurations to a two-dimensional space:

The cannula configuration can be treated as axis-symmetric if a radial homogeneous distribution of the surrounding capillaries is assumed. Besides, the area at the tip of the hollow-fiber is small compared to that of the total length; consequently, its effect on the system performance can be neglected. Therefore, it is not necessary to include the cannula as a domain and the relevant domains are the membrane and the perfusion channel existing between the cannula and the membrane, with the flow entering at the channel from the bottom.

For the single hollow-fiber configuration, it is assumed that the interaction between the probe and the surrounding tissues only reaches a short distance. Therefore, the curvature of the probe is not relevant for the model. Under this simplification, the lumen and the membrane can be assumed to be axis-symmetric rectangular domains with the z-coordinate representing the tube length.

In conclusion, for both model geometries only two cylindrical coordinates are necessary: the z-coordinate represents the length, and the r-coordinate is the distance to the axis of the probe. The only geometric difference between both configurations studied is that for the cannula configuration, there is an inner radius for the perfusion channel greater than zero.

For both configurations, the flow in the perfusion channel is a Poiseuille flow with only a z-component. For an input flow Q, the laminar velocity profile can be obtained from the Navier-Stokes equations using the following assumptions: incompressible, irrotational, and constant properties.

For a single hollow-fiber of inner radius R, the velocity profile for a non-slip condition at the membrane wall and without flow through the wall is given by Eq. 1.

$$U_z(r) = \frac{2\,Q}{\pi} \cdot \frac{(R^2 - r^2)}{R^4} \tag{1}$$

For the hollow-fiber with cannula configuration, the velocity profile in the annular channel with to non-slip condition at the walls placed at R_1 and R_2, Eq. 2 can be derived from a more general form described in [5]:

$$U_z(r) = \\ = \frac{2Q}{\pi} \cdot \frac{R_2^2 \ln\frac{r}{R_1} - R_1^2 \ln\frac{r}{R_2} - r^2 \ln\frac{R_2}{R_1}}{(R_2^2 - R_1^2)^2 \cdot \left(\frac{R_2^2 + R_1^2}{R_2^2 - R_1^2} \ln\frac{R_2}{R_1} - 1\right)} \tag{2}$$

The perfusion flow receives the glucose that has passed through the membrane in radial direction by diffusion. The convective transport has only z-component. A complete description of the transport equations can be seen in [6].

Under proper operating conditions, the volumetric flow through the membrane is negligible. As a consequence, the transport of glucose through the membrane is predominantly diffusive. As the pore size is much larger than the molecule that permeates, the permeability to the glucose can be defined as [7]:

$$P = \kappa \cdot {}^{\epsilon}/_{\tau} \cdot \frac{D_G}{\Delta x_m} \tag{3}$$

where D_G is the glucose diffusivity in the solution inside the pore, Δx_m is the membrane thickness, ε is the porosity, τ is the tortuosity, and κ is a partition coefficient.

The equivalent diffusivity of the glucose in the membrane D_{Gm} is defined as:

$$D_{Gm} = {}^{\epsilon}/_{\tau} \cdot D_S \tag{4}$$

The value of ε/τ for the MD membrane can be obtained from in vitro experiments with glucose solutions.

2.2 Modelling transfer in the tissues

Besides the perfusion channel and the membrane domain, the model include other two concentric layers representing the tissues in contact with the probe (Fig. 2). The normal tissue layer contains plasmatic interstitial fluid that receives glucose from the capillary network.

According to [8], a traumatized layer should be included to account for reaction of the organism against the probe.

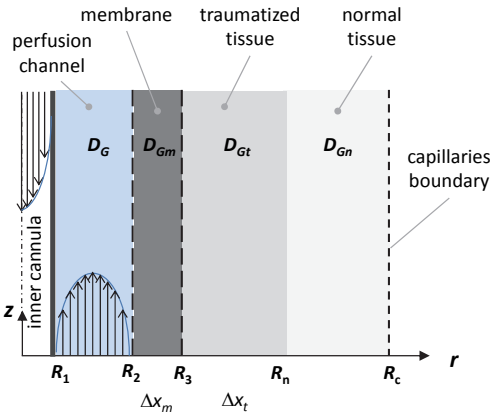

Figure 2. Schematic representation of the layers considered in the model.

It is difficult to model the convective transport in the interstitial tissue domains because the vascular environment is different in each body what implies the impossibility to know the exact velocity profile. However, the convective effects cannot be neglected. To work out this problem, convective transport can be treated as a perturbation [7]. In our case, an effective diffusion coefficient a number of times greater than the value in the plasmatic fluid was used to account for convection.

The transport properties and thickness of the traumatized tissue Δx_t vary in the long term. The value of the effective diffusion coefficient of this layer was the one of the normal tissue multiplied by a factor. In the present development of the model, the evolution of this factor must be experimentally obtained.

The concentration in the external boundary depends on the depth of penetration. The differences between the glucose level in subcutaneous adipose tissue and loose connective tissue are significant. Besides, the depth of each tissue is different in the lateral abdomen and the medial abdomen.

For loose connective tissue the glucose concentration in the plasma tissue (C_{pt}) is similar to the glucose concentration in plasma blood (C_{bp}). For the adipose tissue, the following correlation, valid for $C_{bp} > 4$ mM, was obtained using data from [9]:

$$C_{pt(adipose)} \approx 3\ \text{mM} + 0.25 \cdot C_{bp} \qquad (5)$$

Other correction to be included is that plasma glucose concentrations are 10 to 15% higher than whole blood glucose concentrations (C_{wb}) [10]:

$$C_{bp} \approx 1.1 \cdot C_{wb} \qquad (6)$$

3. Cases studied

Two configurations were defined for this study. The baseline values of their geometric parameters are shown in Table 1. Configuration I was a hollow-fiber with cannula with the same dimension that the one used in [10]. Configuration II was a single hollow-fiber. Both configurations have the same section of the perfusion channel.

Table 1: Geometric parameters for both configurations: I) hollow-fiber with cannula, II) single hollow-fiber

	Definition	**Case**	**Value**
R_1	cannula outer radius	I	75 µm
		II	-
R_2	hollow-fiber inner radius	I	100 µm
		II	66.1 µm
Δx_m	membrane thickness	I, II	10 µm
L	probe length	I, II	15 mm

Table 2 shows the baseline values of the model parameters that were the same for both configurations. The table shows a typical value of the glucose concentration blood and values in the physiological range for the parametric study. The value of the effective diffusivity of glucose in the traumatized tissue was range from 1 to 0.1 times the value of the normal tissue. Arbitrarily, the length of the normal tissue layer was taken equal to two times the length of the traumatized tissue layer. However, this assumption does not significantly affect the results as the value of the

diffusion coefficient in the normal tissue is much greater than the value in the other domains.

Table 2: Baseline values and ranges (in brackets) for model parameters

	Definition	Value or [Range]	Ref.
C_{wb}	glucose concentration in whole blood	5.6 mM [3-16] mM	[11] [9]
$D_{G,i}$	diffusivity of glucose in interstitial fluid	7.3×10^{-6} cm^2/s	[11]
D_{Gm}	effective diffusivity of glucose in the membrane	$0.008 \cdot D_{G,i}$	[12]
u	velocity range for interstitial fluid in normal tissue	[0.1-2] µm/s	[13]
Δx_t	thickness of traumatized tissue layer	20 µm	[8]
α	volume fraction of interstitial phase	0.2	[14]
κ	partition coefficient	1 [0.6 – 1]	[11]

3. Use of COMSOL Multiphysics

3.1 Domains definition

First of all, Eq. 2 was validated in an arbitrary annular channel. As the solution obtained COMSOL do not differ from the analytical solution, Eq. 2 was validated. Therefore, in posterior simulations, for the perfusion channel domain, the flow analytical solution was used in the convection term of the Transport of Dilutes Species in order to reduce the computation time and to improve accuracy. It was also necessary, the diffusion coefficient for glucose in water (Table 1).

For the membrane domain, the effective diffusivity of glucose in the membrane was used.

As we have previously discussed, in the tissue domains the convection effects have not been directly included. Therefore, the Transport of Diluted species model was used without Convection and with an effective diffusion coefficients instead (Table 1).

3.2 Boundary conditions

For all domains, only boundary conditions for glucose concentration were necessary.

The conditions for the perfusion channel domain were the following: For the single hollow-fiber configuration, the conditions was "symmetry" at the axis, and for the hollow-fiber with cannula configuration a "No flux" condition was set at the inner boundary in contact with the cannula. For both configurations, the outer boundary condition was the partition coefficient κ multiplied by the concentration at the membrane side.

For the membrane domain, the inner concentration condition was the concentration in the perfusion channel divided into the partition coefficient. A similar boundary treatment was made at the boundary between the membrane and the traumatized tissue using the partition coefficient. In the boundary between the traumatized tissue and the normal tissue, both domains interchanged the value of concentration at the boundary. The external boundary of the normal tissue domain was set at the glucose concentration in the tissue.

3.4 Meshing

The effects along the radial coordinate are higher than those along the membrane length coordinate z. Therefore, mapped meshing for all entities was appropriate as it allowed a finer estimation of the gradients in the r-coordinate with a smaller number of degrees of freedom. The elements for the perfusion channel domain were radially distributed with a geometric sequence to have smaller element size near to the membrane domain.

3.5 Solving procedure

In all the studies, the direct stationary solver selected was PARDISO. The time dependent problem was solved using the BDF method. The convergence of the problem was good. All the physics could be solved simultaneously without the need of intermediate steps.

4. Results

The model was applied to study the influence of the perfusion rate and the response of the probe to changes in blood glucose concentration and to changes in the resistance of the transport in the traumatized layer.

The average glucose concentration C_{out} at the output of the MD system was calculated using a coupling operator. Then, the glucose recovery could be obtained as the ratio of the dialysate concentration of glucose to the concentration in whole blood:

$$GR = \frac{C_{out}}{C_{wb}} \tag{9}$$

Figure 3 shows the glucose recovery versus the inverse of the perfusion rate for both types of microdialysis probes. It can be seen that glucose recovery was approximately proportional to the inverse of the perfusion flow. Besides, the glucose recovery showed to be almost independent of the glucose concentration in blood (not showed in the figure). A similar result was obtained experimentally by [10]. For the same perfusion flow, the glucose recovery for the hollow-fiber with cannula configuration is greater in spite of both systems having the same channel section. This difference can be explained by the greater area and radial velocity gradients existing in the hollow-fiber with cannula configuration. Nevertheless, the probe radius for the single hollow-fiber configuration is 34% smaller what makes the probe less intrusive.

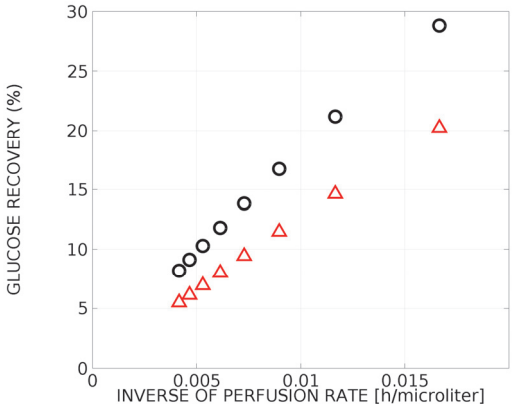

Figure 3. Glucose recovery versus perfusion rate (**O**) hollow-fiber with cannula; (Δ) single hollow-fiber

Figure 4 shows the evolution of glucose recovery after a step change of 25% in the blood glucose concentration respect to the baseline value. It can be seen that both configuration have similar response. The response of both systems stabilizes in less than 20 s.

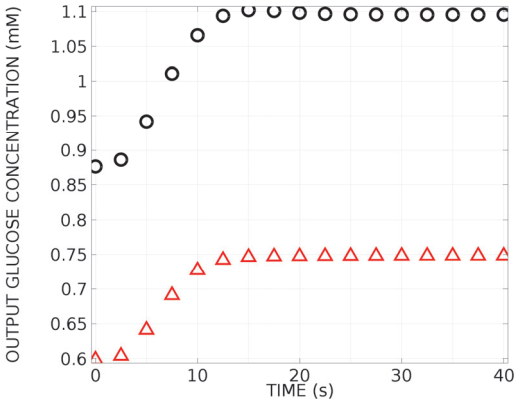

Figure 4. Output glucose concentration after an increment of 25% in blood glucose concentration (**O**) hollow-fiber with cannula; (Δ) single hollow-fiber

Figure 5 shows the evolution of the glucose recovery after an increment of 25% in the perfusion rate. Like in the previous parametric study, the responses of both systems become stable in less than 20 s. The effect of changes in the perfusion flow must be taken into account to correct the glucose measure.

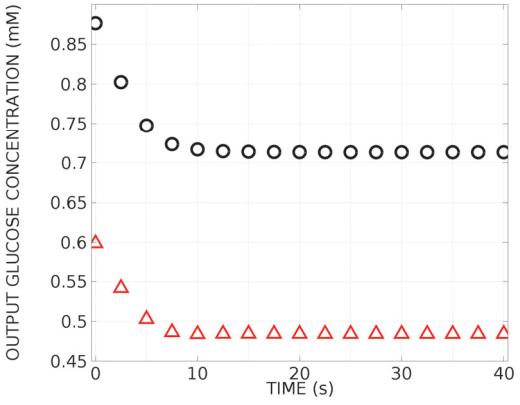

Figure 5. Output glucose concentration after a step change in the perfusion rate from 120 to 150 µL/h. (**O**) hollow-fiber with cannula; (Δ) single hollow-fiber

Figure 6 shows the effect of an increment in the resistance of the traumatized layer. The glucose recovery has been plotted against the ratio of the transport resistance of the traumatized layer to the value of the membrane resistance. It can be seen that when the transport resistance of the traumatized layer becomes 5% greater than that of the membrane, the measured valued is significantly affected. The evolution of the additional resistance to transport should be fitted from experimental data in each case in order to correct the effect on the glucose measure.

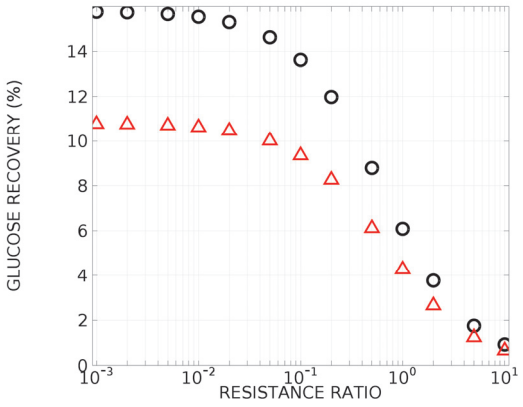

Figure 6. Glucose recovery versus the ratio of the traumatized layer resistance to the membrane resistance. (**O**) hollow-fiber with cannula; (Δ) single hollow-fiber

7. Conclusions

This preliminary approach aims to be the basis for more accurate models useful to improve the performance of continuous glucose monitors by selection of optimal operating conditions (perfusion rate, depth of penetration,...).

The model can also be used to better understand the behavior of a microdialysis probe under different situations like changes in the operating variables or changes in the resistance to transport as a consequence of the inflammatory evolution. Therefore, it can be helpful to develop control models for real devices.

However, in the present development of the model, some biological parameters are uncertain and they must be fitted from experimental data.

Besides its capacity to study the detection of components in tissues like glucose; the microdialysis model can be adapted, with small changes, to study drug delivery by using this technique.

8. References

1. A. Poscia et al, A microdialysis technique for continuous subcutaneous glucose monitoring in diabetic patients (part 1), *Biosensors and bioelectronics*, **18**, 891-898 (2003)
2. C. Höcht et al., Applicability of reverse microdialysis in pharmacological and toxicological studies, *Journal of Pharmacological and Toxicological Methods*, **55**, 3-15 (2007)
3. P. Matzneller, M. Brunner, Recent advances in clinical microdialysis, *Trends in Analytical Chemistry*, **30**, 1497-1504 (2011)
4. E. Wilkins and P. Atanasov, Glucose monitoring: state of the art and future possibilities, *Med. Eng. Phys.*, **18**, 273-288 (1996)
5. Ph. Gittler, Stability of axial Poseuille-Couette flow between concentric cylinders, *Acta Mechanica*, **101**, 1-13 (1993).
6. COMSOL Inc, Chemical Reaction Engineering Module. User's guide, 142-156 (2012)
7. K. Kretsos, G.B. Kasting, A geometrical model of dermal capillary clearance, *Mathematical Biosciences*, **208**, 430–453 (2007)
8. K.C. Chen, Effects of tissue trauma on the characteristics of microdialysis zero-net-flux method sampling neurotransmitters, *Journal of Theoretical Biology*, **238**, 863–881(2006)
9. R.G. Tiessen et al., Glucose gradient differences in subcutaneous tissue of healthy volunteers assessed with ultraslow microdialysis and a nanolitre glucose sensor, *Life Sciences*, **70**, 2457-2466 (2002)
10. Y. Hashiguchi et al., Development of a miniaturized glucose monitoring system by combining a hollow-fiber-type glucose sensor with microdialysis sampling method, *Diabetes care*, **17**, 387-396 (1994)
11. H.R. Clark and T.A. Barbari, Modeling the response time of an in vivo glucose affinity sensor, *Biotechnol. Progress*, **15**, 259-266 (1999)
12. J.D. Zahn et al, Microdialysis microhollow-fibers for continuous medical monitoring, *Biomedical microdevices*, **7**, 59-69 (2005)

13. M.A. Swartz and M.E. Fleury, Interstitial flow and its effects in soft tissues, *Annu. Rev. Biomed. Eng.* **9**, 229–56 (2007)
14. D.Y. Arifin et al., Chemoterapeutic drug transport to brain tumor, *Journal of controlled release*, **137**, 203-210 (2009)

9. Acknowledgements

The authors acknowledge the Universitat Politècnica de Valencia for the Interdisciplinary project PAID/2012/271.